

Electronic Strong Coupling Modifies the Ground-state Intermolecular Interactions in Chlorin Thin Films

Subha Biswas¹, Mainak Mondal^{2#}, Gokul Chandrasekharan^{1#}, Akshay Singh^{2*}, and Anoop Thomas^{1*}

¹Inorganic and Physical Chemistry, Indian Institute of Science, Bengaluru, 560012, India.

²Department of Physics, Indian Institute of Science, Bengaluru, 560012, India.

[#]*These authors contributed equally*

*Correspondence to: aksy@iisc.ac.in; athomas@iisc.ac.in

Keywords: Electronic strong coupling, Vacuum fluctuations, Excitonic interactions, Excimer-like emission, Chlorin

Abstract:

The electronic strong coupling (ESC) of a molecular transition with cavity modes can result in modified excited state photophysics compared to its uncoupled counterparts. Often, such changes are attributed to kinetics effects, overlooking the possible modifications to ground-state intermolecular interactions. The spin-coated films of Chlorin e6 trimethyl ester (Ce6T) provide a platform for studying the role of ESC in dictating photophysics and intermolecular interactions. The preorganization of Ce6T molecules in thin films facilitates intermolecular excitonic interaction, leading to an intense excimer-like emission upon photoexcitation. Interestingly, the ESC of the Ce6T Q-band results in modified luminescence characteristics, where the polaritonic emission dominates over the excimer-like emission. Remarkably, our steady-state, time-resolved emission and the excitation spectral analysis reveal that ESC suppresses the ground-state intermolecular excitonic interactions that otherwise exist in the preorganized Ce6T thin films. These findings will provide valuable insights into the fundamentals of quantum light-matter interactions and coherent energy transport processes.

Main Text:

The electromagnetic field has zero-point energy for its vacuum state, often known as vacuum fluctuations,^{1,2} similar to the zero-point energy of a vibrating molecule. The physical processes, such as spontaneous emission, result from the interaction of matter with the vacuum fluctuation of the electromagnetic field.³ Since free space consists of an infinity of vacuum states, one may overlook the interaction of vacuum fluctuations with the matter.⁴ A photonic device, such as a Fabry-Perot cavity, can confine the photons within the field boundary conditions, enhance the

radiation mode density, and modify the availability.⁴ A molecule inside such a cavity can resonantly exchange energy with the light modes through photons. When the light-matter energy exchange is faster than dissipation, it reaches the strong coupling regime and forms new hybrid light-matter states called the polaritonic states (P+ and P-).⁵ The half-light, half-matter characteristic of the polaritonic state renders unique properties to the system compared to their uncoupled counterparts.^{6,7}

The electronic strong coupling (ESC), or in other words, the hybridization of molecular electronic transition dipoles and cavity modes, has resulted in the modification of photoisomerization,^{8–10} transport,^{11–14} energy transfer,^{15–21} photobleaching,^{22,23} and ultrafast polariton propagation.^{24,25} However, only a few experiments^{26,27} and theoretical^{28–30} studies explored the effect of ESC on the ground-state molecular properties, such as work function²⁶ and free energy.²⁷ Here, by studying the photophysical properties of a spin-coated film of Chlorin e6 trimethyl ester (Ce6T) in non-cavity and under electronic strong coupling conditions, we research the role of ESC in dictating the intermolecular interactions and its effect on the ground and the excited state. The other open question we address here is whether the physical property changes, such as modification to charge-transfer equilibrium^{31,32} and self-assembly^{33–35} observed under collective vibrational strong coupling (VSC),^{36–38} have some parallels under ESC. Our experiments show that the ESC of the Q-band of the Ce6T modifies the ground state intermolecular interactions in Ce6T thin films, leading to the modification of its emission characteristics.

The molecule chlorin e6 trimethyl ester is a derivative of *chlorophyll-a* without the metal center,³⁹ as schematically shown in Figure 1A. Such molecules without the metalation are less likely to form large extended structures like complete H- or J-aggregates.^{40,41} Strong coupling experiments typically require an absorbance of ca. 0.2 or higher for the active material to facilitate the effective energy exchange between the material and cavity to form the polaritonic states.^{5,36} The required absorption is often achieved using a high molecule concentration since the cavity path length must be restricted to a few hundred nm. Accordingly, we prepared a film of Ce6T (400 nm thickness) by spin-coating the solution of Ce6T and polystyrene (PS) in toluene. The absorption spectrum of the Ce6T (16 wt % in PS) film (Figure 1A, solid curve) retains all the spectral features and the intensity ratio of the Soret (405 nm) and Q-bands (668 nm) as in the solution (0.01 mM in toluene; Figure 1A, dotted curve). It indicates the absence of an extended J-aggregate formation as observed in metallated Chlorin, where both the Soret and Q-bands absorbance reduce significantly to form an intense redshifted J-aggregate

band.^{41,42} Interestingly, we notice a new absorption band in the thin film, peaking at 720 nm. The band is observable when the Ce6T amount is above one wt %, and its intensity grows slightly with a concomitant redshift upon increasing the concentration (Figure S1 A and B), suggesting a coupling and delocalization of the transition dipole.⁴³ It indicates that spin coating leads to close packing and assembly of the molecules in the films, albeit the metal center is absent. We verified that the peak is not due to the polystyrene matrix by preparing Ce6T films in non-aromatic poly(methyl methacrylate) (Figure S1). Thus, the absorption at 720 nm is due to the ground-state intermolecular interaction of Ce6T in films, as observed earlier in related systems.^{43–46}

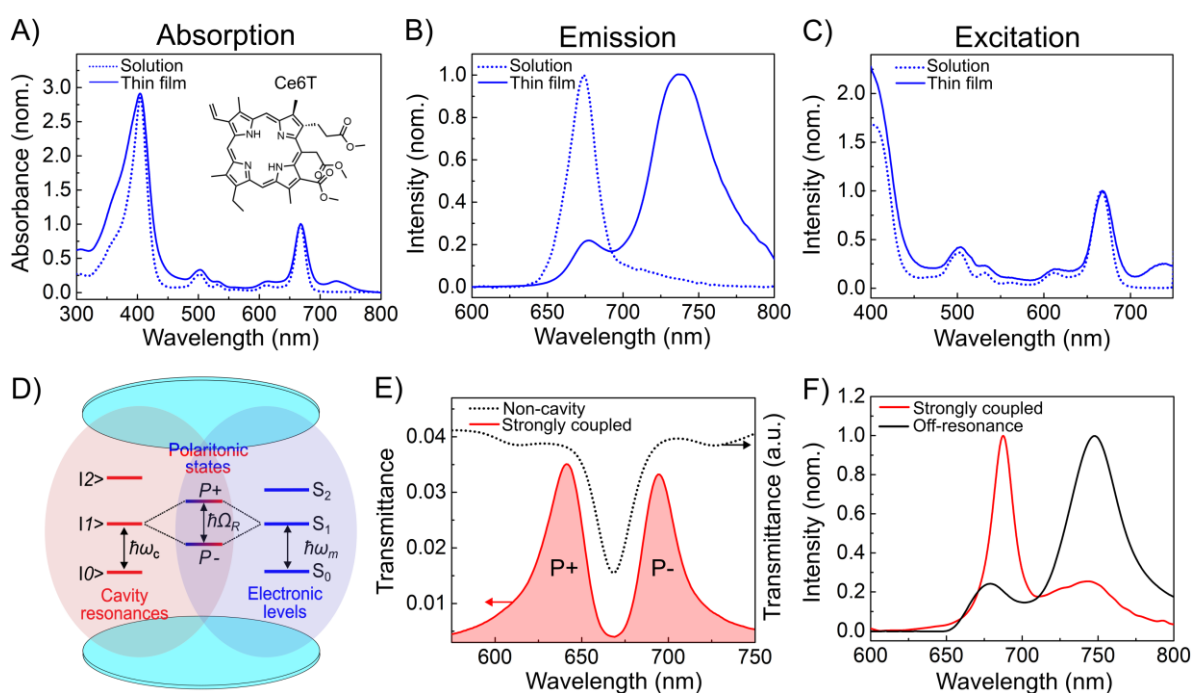


Figure 1: (A) The absorption, (B) the emission ($\lambda_{\text{ex}} = 450$ nm), and (C) the excitation ($\lambda_{\text{em}} = 770$ nm) spectra of Ce6T molecules in toluene (dotted curve) and in thin films (solid curve). The inset in A shows the schematic structure of Ce6T. (D) The schematic illustration of ESC in a Fabry-Perot cavity. (E) The transmittance spectrum (red solid curve with the shaded area) shows the ESC of Ce6T in a Fabry-Perot cavity. P+ and P- denote the polaritonic states. The black dotted curve indicates the transmission spectrum of non-cavity Ce6T. (F) The emission ($\lambda_{\text{ex}} = 450$ nm) spectrum of Ce6T under ESC (red curve) and in an off-resonance cavity (black curve). The λ_{ex} and λ_{em} represent the excitation and emission wavelength, respectively.

The Ce6T molecules in toluene show a fluorescence maximum at 674 nm and a shoulder at 720 nm (Figure 1B, dotted curve, $\lambda_{\text{ex}} = 450$ nm) with the same emission lifetime (5 ns; Figure S2), confirming their identical origin. In contrast, the emission maximum in the thin film is at 740 nm, whose intensity is four times larger than the other emission peak at 674 nm (Figure 1B, solid curve). The 674 nm emission band decays immediately upon excitation with a

lifetime of 790 ± 30 ps. In contrast, the 740 nm band forms with a mono-exponential rise time of 200 ± 10 ps and decays in 1.1 ± 0.1 ns. We attribute the 674 nm emission to the Ce6T monomer. Further, we conducted the excitation spectral analysis to understand the origin of the long-lived, intense, broad, vibrationless emission band. The excitation spectrum of the thin film Ce6T, recorded by following the emission at the tail (770 nm) of the 740 nm band (Figure 1C, solid curve), matched with the thin film absorption spectrum, suggesting that the 740 nm band could be arising from an excimer-like state.^{43,47} We call the 740 nm emission excimer-like, in line with the earlier reports,^{43,48,49} because it shows the emission characteristics of a conventional excimer, while we cannot exclude their ground-state interactions as evidenced by the 720 nm peak. The spin coating ensures the proximity of Ce6T molecules in the thin film, leading to preorganization and the coupling of transition dipoles, subsequently facilitating rapid excimer-like state formation upon photoexcitation. This observation correlates with organized perylene- and pyrene-based molecular systems.^{43,47-50}

The photophysical characteristics exhibited by Ce6T in thin films present a unique opportunity to probe their ground-state intermolecular interactions under ESC. In typical ESC experiments, the J-aggregate transition dipoles are often strongly coupled with the cavity modes.⁵ Then, it is not apparent how the ESC of the monomer transition will affect the excitonic interactions of the assembled state. In this regard, the Ce6T films are distinct, as the molecules are not in a complete H- or J-aggregate form but in a preorganized state to give an observable excitonic coupling band at 720 nm. It allows us to strongly couple the Q-band transition and follow the effect of ESC on the excitonic interaction and the subsequent excimer-like state emission.

To explore the role of cavity ESC on the intermolecular interaction and the emission from an excimer-like state, we strongly coupled the intense Q-band of Ce6T ($\lambda_{\text{max}} = 668$ nm; 1.85 eV) by placing spin-coated Ce6T films in a Fabry-Perot cavity made of two Al mirrors of 30 nm thickness (See scheme in Figure 1D). The concentration of the Ce6T (16 wt% in PS) and film thickness (400 nm) were optimized to strongly couple the Q-band with the cavity resonance (second mode). See Supporting Information for details. The appearance of two new peaks corresponding to the polaritonic states, P+ at 642 nm (1.78 eV) and P- at 696 nm (1.93 eV), in the transmission spectrum indicates the ESC of the Q-band (Figure 1E, red shaded curve). The larger Rabi splitting energy (150 meV) than the width of the cavity mode (120 ± 5 meV) and the Q-band (60 meV) confirms the ESC.⁵¹ We also prepared off-resonance and one-mirror (half) cavities to the Q-band by varying the cavity path length to compare with the strongly coupled Ce6T (Figure S3).

We then analyzed the emission properties of the strongly coupled Ce6T by exciting at 450 nm. The Ce6T under ESC (Figure 1F red curve) shows an intense narrow monomer-like ($\lambda_{\text{max}} = 690$ nm) and a weak excimer-like emission band ($\lambda_{\text{max}} = 740$ nm). The monomer-like emission band disperses with varying angles of incidence, indicating its polaritonic nature (Figure S4), and we attribute its origin to the P- state. The slight blue shift of the P- emission compared to the absorption has been a feature in many experiments.^{51–55} In strongly coupled systems consisting of molecules at room temperature, the emission from the P+ state is rarely observed due to the nonradiative decay to the lower energy levels.^{55–58} Interestingly, the excimer-like emission (Figure S4) showed no dispersive characteristics, indicating a non-polaritonic nature.^{59,60} In the off-resonance (Figure 1F, black curve), detuned, and one-mirror cavities (Figure S3), the emission spectra resemble the one in non-cavity, confirming that the emission modification originates from the ESC of Q-bands.

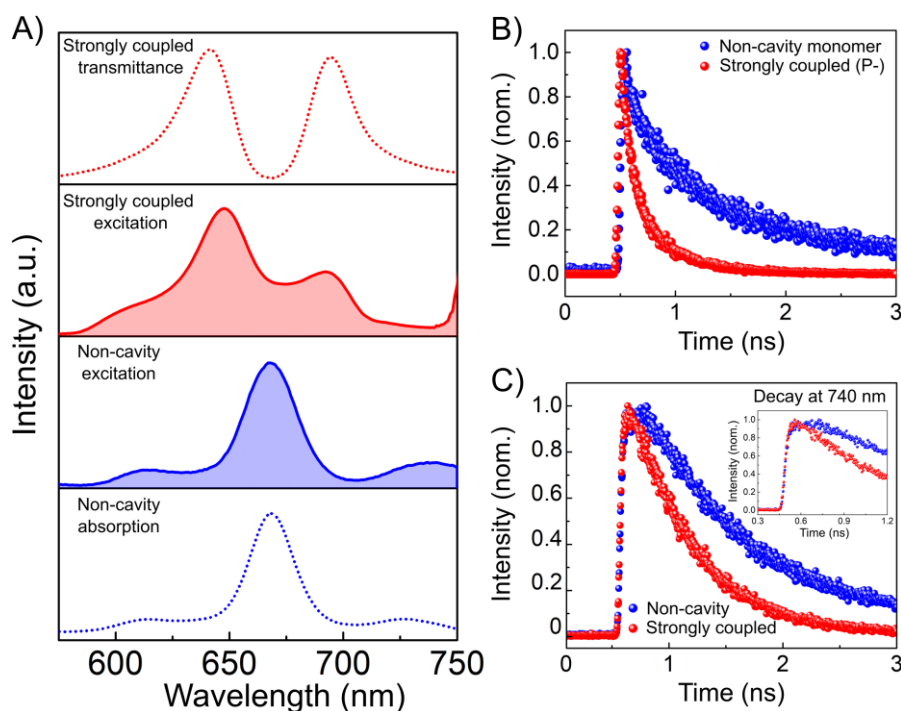


Figure 2: (A) The top panel shows the excitation spectrum of Ce6T under ESC (red shaded curve; $\lambda_{\text{em}} = 770$ nm) and compares it with the transmittance spectrum under ESC (red dotted curve). The bottom panel shows the excitation spectrum of non-cavity Ce6T (blue shaded curve; $\lambda_{\text{em}} = 770$ nm) compared to its absorption spectrum (blue dotted curve). (B) The emission decay profile of Ce6T under ESC (red spheres; collected at 690 nm) and non-cavity (blue spheres; recorded at 674 nm) upon excitation at 450 nm. (C) The emission decay profile of Ce6T recorded at 740 nm, under ESC (red spheres) and in non-cavity (blue spheres). The zoom of the decay profile in the inset shows the presence and absence of rise time in non-cavity and under ESC, respectively.

To better understand the origin of the weak excimer-like emission band under ESC, we recorded the excitation spectrum by collecting the emission response at the red tail of the emission band (770 nm). The excitation spectrum exhibited strong peaks at P+ (648 nm) and P- (686 nm) positions and a weak transition at 612 nm (Figure 2A, top panel). It is surprising that the excimer-like emission band under ESC with the non-polaritonic character originates from the excitation of the polaritonic states. Interestingly, the contribution of the P+ state to the emission is relatively more significant than P-, as seen earlier in other experiments^{54,61}, and suggests that excitation of the polaritonic states can have different contributions to the emission. The other remarkable feature of the excitation spectrum under ESC is the absence of the excitonic coupling band at 720 nm, in contrast to the absorption and excitation spectra of the non-cavity Ce6T (Figure 2A, blue dotted and shaded curve). The excitation spectra of the off-resonance, detuned, and one-mirror cavities under the same experimental conditions (Figure S5) were similar to that of non-cavity, confirming that the above observation is unique to ESC. The absence of the 720 nm band in the excitation spectrum under ESC suggests that the intermolecular interaction is either absent under ESC or does not contribute to the non-dispersive emission at 740 nm, even though the molecules are preorganized in the film state. The absence of the 720 nm peak is also not due to any instrumental limitation when measuring the cavity, as we clearly see the weak contribution of the 612 nm band towards the 740 nm emission, and it also rules out the possibility of a cavity filter effect. Thus, the excitation spectral studies indicate that the weak, non-dispersive 740 nm emission under ESC differs from the excimer-like emission of non-cavity. In other words, the 740 nm emission band under ESC is not that of the Ce6T molecules forming excimer-like states.

Further, we analyzed the decay of the polaritonic and excimer-like emission bands under ESC. The P- emission decays nearly three times faster (240 ± 30 ps; red spheres, Figure 2B) than the 740 nm band under ESC (780 ± 20 ps; red spheres, Figure 2C), and the monomer emission of non-cavity Ce6T (790 ± 30 ps; blue spheres, Figure 2B). The absence of the rise and the shorter lifetime compared to the non-cavity excimer-like emission (1.1 ± 0.1 ns; blue spheres, Figure 2C) further shows that the origin and the character of the 740 nm emission under ESC is different from the excimer-like emission that could arise from uncoupled preorganized Ce6T molecules. Interestingly, the decay characteristics of the 740 nm emission of the strongly coupled Ce6T are closer to the non-cavity monomer. Once again, the emission decay of the off-resonance, detuned, and one-mirror cavities was identical to that of non-cavity Ce6T molecules (Figure S3). Thus, the time-resolved emission analysis shows that the ESC opens up

an efficient ultrafast pathway for the Ce6T molecules to emit through the polaritonic state. In contrast, the 740 nm emission under ESC originates from a monomer-like excited state.

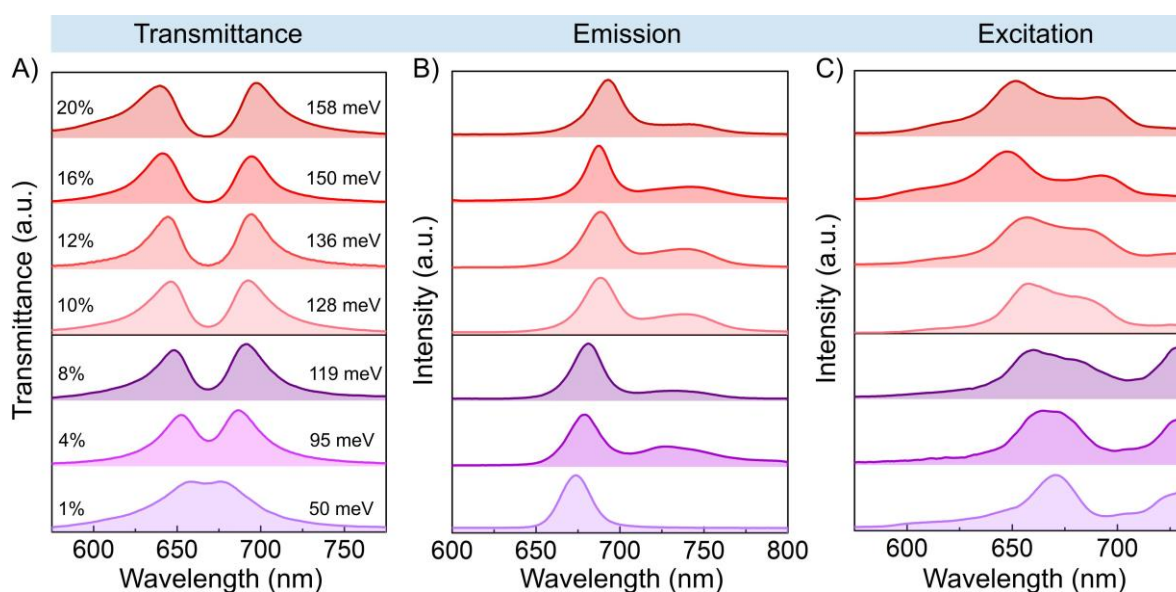


Figure 3: (A) The transmission spectra of the cavities show the changes in the Rabi splitting energy as a function of the varying concentration of Ce6T (wt % of Ce6T in PS is indicated in the figure). The violet-shaded curves are under the weak coupling regime, while the red-shaded curves correspond to the ESC regime. Modulation of (B) the emission and (C) the excitation spectra of Ce6T under weak coupling (violet-shaded curves) and under ESC (red-shaded curves). The cavities were excited at 450 nm for emission measurements, and for the excitation spectra recording, we collected the emission at 770 nm.

The weak coupling of light and matter can also modulate the emission properties. For instance, a red detuned cavity with its mode ($\hbar\omega_c = 750$ nm) in resonance with the Ce6T excimer-like band enhances the latter (Figure S3). However, the presence of the 720 nm excitonic coupling band in the excitation spectrum of the red-detuned cavity indicates that intermolecular interactions in the weak and strong coupling regimes are different. Since the Rabi splitting energy varies with the square root of the number of coupled molecules,⁵ we prepared cavities with varying concentrations of Ce6T to investigate the role of weak and strong coupling and monitored the photophysics. We ranged the Ce6T concentration from 1 wt % to 20 wt % while maintaining the cavity path length. Figure 3A shows that Ce6T reaches the ESC regime (red curves) when the concentration is ≥ 10 wt%. The Rabi splitting energy at 10 wt % of Ce6T (128 ± 5 meV) is larger than the cavity mode width (120 ± 5 meV) and the Q-band of Ce6T (60 meV). For other lower Ce6T concentrations (Figure 3A, violet curves), the splitting is less than the FWHM of the cavity modes (120 ± 5 meV) and is, therefore, in a weak coupling regime. The plot of the Rabi splitting energy against the square root of Ce6T concentration also

shows a distinct variation of slopes below and above 10 wt % of Ce6T, indicating a transition from weak to strong light-matter coupling (Figure S6).

Interestingly, the monomer/polaritonic emission is more intense in weak and strong coupling regimes, as seen in Figure 3B. The cavity mode in the weak coupling regime almost resonates with the Ce6T emission as the Stokes shift is only 6 nm. Hence, the Purcell effect⁶² can enhance the monomer emission in the weak coupling regime.⁵¹ However, for 1 and 4 wt % Ce6T, the monomer emission dominates the excimer even in non-cavity (Figure S7); hence, the weak coupling has less significance. In the ESC regime, the P- emission peaks are ≥ 690 nm, which is 16 nm redshifted compared to the monomer emission band. Therefore, the intense polaritonic emission is not just due to modifying the radiation mode density at the emission wavelength. We observe a weak redshifted emission band in all the concentration regimes. The excitation spectral response collected at 770 nm, far from the P- emission peak or cavity modes, conspicuously distinguishes the effect of weak and strong coupling on Ce6T films. In the weak coupling regime (Figure 3C, violet shaded curves), the excitation spectra consist of all the bands as in non-cavity (Q-bands and excitonic coupling band at 720 nm), and the primary excitation responsible for the emission at 770 nm is the 668 nm Q-band. These observations confirm that the weak coupling interactions only enhance the emission at the monomeric region without affecting the intermolecular excitonic interaction. Remarkably, in the ESC regime, the primary excitation is through the polaritonic bands, and more interestingly, the 720 nm excitonic coupling band is absent (Figure 3C, red-shaded curves). Thus, the light-matter hybridization under ESC modifies the formation of an excimer-like state by altering the intermolecular interaction in the preorganized state. In all the curves, the P+ intensity is higher than that of P-, suggesting that the two polaritonic states have different contributions toward the 740 nm emission. It also indicates that direct excitation of the two polaritonic states may not result in identical outcomes.^{54,55,57,61}

We then analyzed the emission decay in the weak and strong coupling regime and compared it with the non-cavity. The emission lifetime of the monomer and the excimer-like emission decreased steadily in the weak coupling regime (Figure 4 A, red spheres and open circles; Rabi splitting energy < 120 meV) and in non-cavity (Figure S8), indicative of the enhanced intermolecular interaction with the increase in the concentration of Ce6T. In contrast, under ESC, the lifetime of the polaritonic state (240 ± 30 ps) and the 740 nm band (850 ± 70 ps) remained nearly the same (Figure 4A and S9). The other remarkable aspect was the presence (weak coupling) and the absence (under ESC) of rise time in the emission decay ($\lambda_{em} = 740$

nm), showing the distinct character of the 740 nm emission in the weak and strong light-matter coupling regimes.

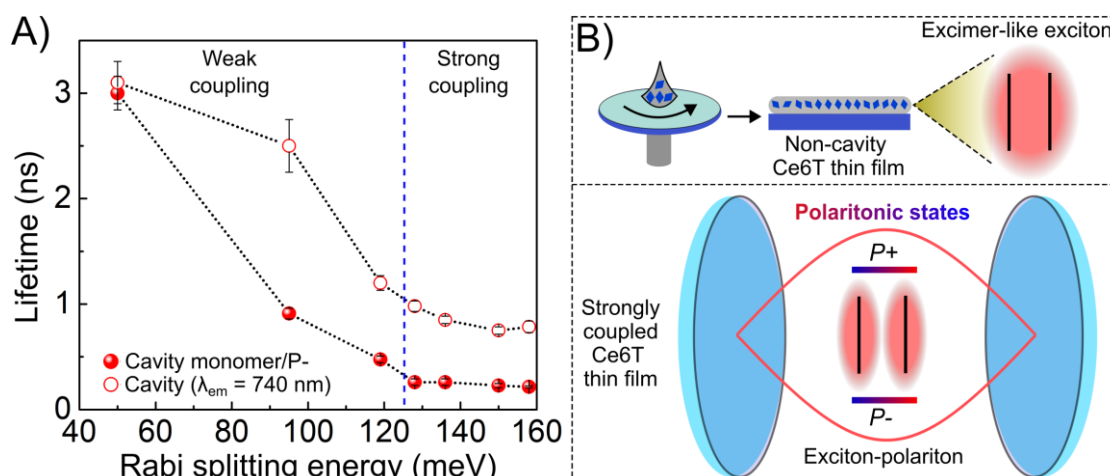


Figure 4: (A) The emission lifetime of Ce6T under ESC as a function of Rabi splitting energy. The lifetime of the cavity monomer-like emission ($P-$ state under ESC) is shown in red spheres, and that of the 740 nm band is shown in red open circles. (B) Schematic illustration of the excimer-like exciton formed in non-cavity Ce6T films upon spin coating (top panel) and the non-interacting exciton polaritons under ESC (bottom panel).

Since an excimer formation is associated with a rise time,⁴⁷ it is clear that the emission at 740 nm in the weakly coupled samples arises from the excimer-like states. Therefore, it is reasonable to say that the excitonic coupling band (720 nm) in the absorption and excitation spectra of non-cavity is a signature of the ground-state intermolecular interactions in the preorganized Ce6T films that facilitate the excimer-like state formation (Figure 4B, top panel). Then, the absence of both the excitonic coupling band in the excitation spectrum and the rise time at 740 nm under ESC reveals that the hybrid-light matter states suppress the transition dipole interactions between Ce6T even in the concentrated thin film state, preventing the excimer-like state formation as schematically shown in the bottom panel of Figure 4B. In fluorescence quenching experiments, an invariant lifetime of the fluorophore typically suggests a static quenching, in which the quencher forms a ground-state complex with the fluorophore.⁶³ Drawing parallels, the hybrid light-matter states under ESC modify the properties of preorganized Ce6T like a ground-state complex formation. On the other hand, the cavity-matter interaction in the weak coupling regime could be regarded as parallel to dynamic quenching, where the fluorophore interacts with the quencher in the excited state, decreasing the emission lifetime.⁶³ Therefore, the non-variant emission decay under ESC suggests that ESC modifies the ground state before light excitation. Such modifications to the ground-state intermolecular interaction may also result in Free energy changes, as observed earlier.²⁷

Our experiments reveal remarkable features of strongly coupled Ce6T: (i) the modification of emission characteristics, (ii) the absence of the 720 nm excitonic coupling band in the excitation spectrum, and (iii) the invariant emission lifetime. We show that although both weak and strong coupling changes the emission characteristics, the underlying mechanism of action is distinctly different. The enhanced polaritonic emission under ESC is not just due to the Purcell factor but is related to modifying the ground state intermolecular interaction under ESC. The collective strong coupling of the Ce6T Q-band and cavity modes suppresses the ground-state excitonic interaction of Ce6T molecules. It leads to the subsequent quenching of an excimer-like state, which otherwise exists in the preorganized thin film. The invariant lifetime of polaritonic emission in the ESC regime suggests that the onset of ESC modifies the emission characteristics by establishing newer or modifying the existing intermolecular interaction factors. Our observation aligns with recent theoretical studies^{29,64} that show that the competition between short-range intermolecular forces and photonic correlation under collective strong coupling induces local changes to the transition density and polarizability of the solvation shell. Although VSC has been shown to modify the solvent polarity,⁶⁵ dispersion forces,³² and self-assembly,^{33,35,34,66} ours is the first experiment, to our knowledge, to show that ESC can change the ground-state intermolecular interactions. Thus, we argue that the mode of action under collective vibrational or electronic strong coupling can be similar.

The nature of the 740 nm emission band under ESC is even more intriguing. The absence of rise time indicates that it is not an uncoupled molecule emitting from the excimer-like state. However, the non-dispersive character of the emission suggests that the emission does not arise from the polaritonic states.³⁰ It can be thought that the 740 nm emission is emerging from an energy state below the P- in accordance with the 720 nm excitonic coupling band in absorption. Then, there can be a cascade of population transfer from P+ to P- and subsequently to the lower-lying emissive state. However, the excitation spectrum under ESC conspicuously shows that the 740 nm emission is mainly due to the excitation of the polaritonic states, and the 720 nm band is absent. Therefore, the 740 nm emission under ESC could originate from the dark states.³⁰ Spectroscopically, the dark state levels should be between the polaritonic energy levels. However, Scholes et al. show that entropy reordering can change the free energies of polaritonic states, placing the dark state below the P+ and P- in terms of free energy, allowing the population to transfer to the dark state, from which it can emit.³⁰ This scenario correlates well with the non-dispersive character of the 740 nm emission, the absence of rise time, the excitation spectrum, and the lifetime studies under ESC. Thus, adopting Scholes et al.,³⁰ the

740 nm emission band under ESC corresponds to the emission of dark states, which gets populated through the polaritonic states.

Our experiment under ESC, together with other VSC studies,^{32–35,65–67} points to the possibility that collective light-matter strong coupling can alter the weak intermolecular interaction forces. Such modifications to the inter- or intramolecular interactions can indeed cause changes to the molecular organization^{33–35} and alignment of magnetic spin,⁶⁸ change the metal to insulator transitions,⁶⁹ and may open up new conducting pathways.^{11–13,70}

Acknowledgments

We thank the Department of Inorganic and Physical Chemistry, IISc, and Prof. S. Ramakrishnan for providing access to instrumentation facilities. We thank Ms. Rashmita (visiting student from NISER Bhubaneswar) for her help. SB and MM thank the Prime Minister's Research Fellowship (PMRF) for the Ph.D. fellowship. GC thanks SERB for the fellowship. AS thanks IISc for the start-up grant and Infosys Foundation for Young Investigator Award. AT thanks IISc for the start-up grant (IE/CARE-21-0321 and SR/MHRD-20-0039), DST-SERB for the core research grant (CRG/2021/002396), and Infosys Foundation for Young Investigator Award (FG/OTHR-21-1050). We thank Dr. Veerbhadrarao Kaliginedi for the helpful discussion.

Author contributions

All the authors contributed to the results presented in the paper. All the authors analyzed the data discussed together and wrote the manuscript.

Competing interests

The authors declare no competing interests.

Additional Information

Supplementary Information

References:

- (1) Milonni, P. W., *The Quantum Vacuum*; Academic Press: San Diego, 1994. <https://doi.org/10.1016/B978-0-08-057149-2.50001-1>.
- (2) Fox, M.; Fox, M. *Quantum Optics: An Introduction*; Oxford Master Series in Physics; Oxford University Press: Oxford, New York, 2006.
- (3) Milonni, P. W. Why Spontaneous Emission? *Am. J. Phys.* **1984**, *52* (4), 340–343. <https://doi.org/10.1119/1.13886>.
- (4) Haroche, S.; Kleppner, D. Cavity Quantum Electrodynamics. *Phys. Today* **1989**, *42* (1), 24. <https://doi.org/10.1063/1.881201>.
- (5) Ebbesen, T. W. Hybrid Light–Matter States in a Molecular and Material Science Perspective. *Acc. Chem. Res.* **2016**, *49* (11), 2403–2412. <https://doi.org/10.1021/acs.accounts.6b00295>.

- (6) Garcia-Vidal, F. J.; Ciuti, C.; Ebbesen, T. W. Manipulating Matter by Strong Coupling to Vacuum Fields. *Science* **2021**, *373* (6551). <https://doi.org/10.1126/science.abd0336>.
- (7) Hirai, K.; Hutchison, J. A.; Uji-i, H. Molecular Chemistry in Cavity Strong Coupling. *Chem. Rev.* **2023**. <https://doi.org/10.1021/acs.chemrev.2c00748>.
- (8) Hutchison, J. A.; Schwartz, T.; Genet, C.; Devaux, E.; Ebbesen, T. W. Modifying Chemical Landscapes by Coupling to Vacuum Fields. *Angew. Chem. Int. Ed.* **2012**, *51* (7), 1592–1596. <https://doi.org/10.1002/anie.201107033>.
- (9) Zeng, H.; Pérez-Sánchez, J. B.; Eckdahl, C. T.; Liu, P.; Chang, W. J.; Weiss, E. A.; Kalow, J. A.; Yuen-Zhou, J.; Stern, N. P. Control of Photoswitching Kinetics with Strong Light–Matter Coupling in a Cavity. *J. Am. Chem. Soc.* **2023**. <https://doi.org/10.1021/jacs.3c04254>.
- (10) Galego, J.; Garcia-Vidal, F. J.; Feist, J. Suppressing Photochemical Reactions with Quantized Light Fields. *Nat. Commun.* **2016**, *7*, 13841. <https://doi.org/10.1038/ncomms13841>.
- (11) Orgiu, E.; George, J.; Hutchison, J. A.; Devaux, E.; Dayen, J. F.; Doudin, B.; Stellacci, F.; Genet, C.; Schachenmayer, J.; Genes, C.; Pupillo, G.; Samorì, P.; Ebbesen, T. W. Conductivity in Organic Semiconductors Hybridized with the Vacuum Field. *Nat. Mater.* **2015**, *14* (11), 1123–1129. <https://doi.org/10.1038/nmat4392>.
- (12) Krainova, N.; Grede, A. J.; Tsokkou, D.; Banerji, N.; Giebink, N. C. Polaron Photoconductivity in the Weak and Strong Light-Matter Coupling Regime. *Phys. Rev. Lett.* **2020**, *124* (17), 177401. <https://doi.org/10.1103/PhysRevLett.124.177401>.
- (13) Bhatt, P.; Kaur, K.; George, J. Enhanced Charge Transport in Two-Dimensional Materials through Light–Matter Strong Coupling. *ACS Nano* **2021**, *15* (8), 13616–13622. <https://doi.org/10.1021/acsnano.1c04544>.
- (14) Hagenmüller, D.; Schachenmayer, J.; Schütz, S.; Genes, C.; Pupillo, G. Cavity-Enhanced Transport of Charge. *Phys. Rev. Lett.* **2017**, *119* (22), 223601. <https://doi.org/10.1103/PhysRevLett.119.223601>.
- (15) Coles, D. M.; Somaschi, N.; Michetti, P.; Clark, C.; Lagoudakis, P. G.; Savvidis, P. G.; Lidzey, D. G. Polariton-Mediated Energy Transfer between Organic Dyes in a Strongly Coupled Optical Microcavity. *Nat. Mater.* **2014**, *13* (7), 712–719. <https://doi.org/10.1038/nmat3950>.
- (16) Zhong, X.; Chervy, T.; Wang, S.; George, J.; Thomas, A.; Hutchison, J. A.; Devaux, E.; Genet, C.; Ebbesen, T. W. Non-Radiative Energy Transfer Mediated by Hybrid Light-Matter States. *Angew. Chem. Int. Ed.* **2016**, *55* (21), 6202–6206. <https://doi.org/10.1002/anie.201600428>.
- (17) Zhong, X.; Chervy, T.; Zhang, L.; Thomas, A.; George, J.; Genet, C.; Hutchison, J. A.; Ebbesen, T. W. Energy Transfer between Spatially Separated Entangled Molecules. *Angew. Chem. Int. Ed.* **2017**, *56* (31), 9034–9038. <https://doi.org/10.1002/anie.201703539>.
- (18) Garcia-Vidal, F. J.; Feist, J. Long-Distance Operator for Energy Transfer. *Science* **2017**, *357* (6358), 1357–1358. <https://doi.org/10.1126/science.aao4268>.
- (19) Akulov, K.; Bochman, D.; Golombek, A.; Schwartz, T. Long-Distance Resonant Energy Transfer Mediated by Hybrid Plasmonic–Photonic Modes. *J. Phys. Chem. C* **2018**, *122* (28), 15853–15860. <https://doi.org/10.1021/acs.jpcc.8b03030>.

- (20) Tibben, D. J.; Bonin, G. O.; Cho, I.; Lakhwani, G.; Hutchison, J.; Gómez, D. E. Molecular Energy Transfer under the Strong Light–Matter Interaction Regime. *Chem. Rev.* **2023**, *123* (13), 8044–8068. <https://doi.org/10.1021/acs.chemrev.2c00702>.
- (21) Martínez-Martínez, L. A.; Du, M.; F. Ribeiro, R.; Kéna-Cohen, S.; Yuen-Zhou, J. Polariton-Assisted Singlet Fission in Acene Aggregates. *J. Phys. Chem. Lett.* **2018**, *9* (8), 1951–1957. <https://doi.org/10.1021/acs.jpcclett.8b00008>.
- (22) Munkhbat, B.; Wersäll, M.; Baranov, D. G.; Antosiewicz, T. J.; Shegai, T. Suppression of Photo-Oxidation of Organic Chromophores by Strong Coupling to Plasmonic Nanoantennas. *Sci. Adv.* **2018**, *4* (7), eaas9552. <https://doi.org/10.1126/sciadv.aas9552>.
- (23) Peters, V. N.; Faruk, M. O.; Asane, J.; Alexander, R.; Peters, D. A.; Prayakarao, S.; Rout, S.; Noginov, M. A. Effect of Strong Coupling on Photodegradation of the Semiconducting Polymer P3HT. *Optica* **2019**, *6* (3), 318–325. <https://doi.org/10.1364/OPTICA.6.000318>.
- (24) Balasubrahmaniam, M.; Simkhovich, A.; Golombek, A.; Sandik, G.; Ankonina, G.; Schwartz, T. From Enhanced Diffusion to Ultrafast Ballistic Motion of Hybrid Light–Matter Excitations. *Nat. Mater.* **2023**, *22* (3), 338–344. <https://doi.org/10.1038/s41563-022-01463-3>.
- (25) Xu, D.; Mandal, A.; Baxter, J. M.; Cheng, S.-W.; Lee, I.; Su, H.; Liu, S.; Reichman, D. R.; Delor, M. Ultrafast Imaging of Polariton Propagation and Interactions. *Nat. Commun.* **2023**, *14* (1), 3881. <https://doi.org/10.1038/s41467-023-39550-x>.
- (26) Hutchison, J. A.; Liscio, A.; Schwartz, T.; Canaguier-Durand, A.; Genet, C.; Palermo, V.; Samorì, P.; Ebbesen, T. W. Tuning the Work-Function Via Strong Coupling. *Adv. Mater.* **2013**, *25* (17), 2481–2485. <https://doi.org/10.1002/adma.201203682>.
- (27) Canaguier-Durand, A.; Devaux, E.; George, J.; Pang, Y.; Hutchison, J. A.; Schwartz, T.; Genet, C.; Wilhelms, N.; Lehn, J.-M.; Ebbesen, T. W. Thermodynamics of Molecules Strongly Coupled to the Vacuum Field. *Angew. Chem. Int. Ed.* **2013**, *52* (40), 10533–10536. <https://doi.org/10.1002/anie.201301861>.
- (28) Scholes, G. D. Emergence of Collective Coherent States from Strong-Light Coupling of Disordered Systems. *J. Phys. Chem. A* **2021**, *125* (31), 6739–6750. <https://doi.org/10.1021/acs.jpca.1c05400>.
- (29) Haugland, T. S.; Schäfer, C.; Ronca, E.; Rubio, A.; Koch, H. Intermolecular Interactions in Optical Cavities: An Ab Initio QED Study. *J. Chem. Phys.* **2021**, *154* (9), 094113. <https://doi.org/10.1063/5.0039256>.
- (30) Scholes, G. D.; DelPo, C. A.; Kudisch, B. Entropy Reorders Polariton States. *J. Phys. Chem. Lett.* **2020**, *11* (15), 6389–6395. <https://doi.org/10.1021/acs.jpcclett.0c02000>.
- (31) Pang, Y.; Thomas, A.; Nagarajan, K.; Vergauwe, R. M. A.; Joseph, K.; Patrahau, B.; Wang, K.; Genet, C.; Ebbesen, T. W. On the Role of Symmetry in Vibrational Strong Coupling: The Case of Charge-Transfer Complexation. *Angew. Chem. Int. Ed.* **2020**, *59* (26), 10436–10440. <https://doi.org/10.1002/anie.202002527>.
- (32) Ebbesen, T.; Patrahau, B.; Piejko, M.; Mayer, R.; Antheaume, C.; Sangchai, T.; Ragazzon, G.; Jayachandran, A.; Devaux, E.; Genet, C.; Moran, J. Direct Observation of Polaritonic Chemistry by Nuclear Magnetic Resonance Spectroscopy. ChemRxiv December 8, 2023. <https://doi.org/10.26434/chemrxiv-2023-349f5>.

- (33) Joseph, K.; Kushida, S.; Smarsly, E.; Ihiwakrim, D.; Thomas, A.; Paravicini-Bagliani, G. L.; Nagarajan, K.; Vergauwe, R.; Devaux, E.; Ersen, O.; Bunz, U. H. F.; Ebbesen, T. W. Supramolecular Assembly of Conjugated Polymers under Vibrational Strong Coupling. *Angew. Chem. Int. Ed.* **2021**, *60* (36), 19665–19670. <https://doi.org/10.1002/anie.202105840>.
- (34) Sandeep, K.; Joseph, K.; Gautier, J.; Nagarajan, K.; Sujith, M.; Thomas, K. G.; Ebbesen, T. W. Manipulating the Self-Assembly of Phenyleneethynylenes under Vibrational Strong Coupling. *J. Phys. Chem. Lett.* **2022**, *13* (5), 1209–1214. <https://doi.org/10.1021/acs.jpcclett.1c03893>.
- (35) Hirai, K.; Ishikawa, H.; Chervy, T.; Hutchison, J. A.; Uji-i, H. Selective Crystallization via Vibrational Strong Coupling. *Chem. Sci.* **2021**, *12* (36), 11986–11994. <https://doi.org/10.1039/D1SC03706D>.
- (36) Nagarajan, K.; Thomas, A.; Ebbesen, T. W. Chemistry under Vibrational Strong Coupling. *J. Am. Chem. Soc.* **2021**, *143* (41), 16877–16889. <https://doi.org/10.1021/jacs.1c07420>.
- (37) Dunkelberger, A. D.; Simpkins, B. S.; Vurgaftman, I.; Owrutsky, J. C. Vibration-Cavity Polariton Chemistry and Dynamics. *Annu. Rev. Phys. Chem.* **2022**, *73* (1), 429–451. <https://doi.org/10.1146/annurev-physchem-082620-014627>.
- (38) Hirai, K.; Hutchison, J. A.; Uji-i, H. Recent Progress in Vibropolaritonic Chemistry. *ChemPlusChem* **2020**, *85* (9), 1981–1988. <https://doi.org/10.1002/cplu.202000411>.
- (39) Nagano, Y.; Ogasawara, S.; Tamiaki, H. Regioisomeric Synthesis of Chlorin-E6 Dimethyl Esters and Their Optical Properties. *J. Porphyr. Phthalocyanines* **2018**. <https://doi.org/10.1142/S1088424618501043>.
- (40) Tamiaki, H. Supramolecular Structure in Extramembraneous Antennae of Green Photosynthetic Bacteria. *Coord. Chem. Rev.* **1996**, *148*, 183–197. [https://doi.org/10.1016/0010-8545\(95\)01188-9](https://doi.org/10.1016/0010-8545(95)01188-9).
- (41) Balaban, T. S.; Tamiaki, H.; Holzwarth, A. R. Chlorins Programmed for Self-Assembly. In *Supramolecular Dye Chemistry*; Würthner, F., Ed.; Topics in Current Chemistry; Springer: Berlin, Heidelberg, 2005; pp 1–38. <https://doi.org/10.1007/b137480>.
- (42) Tamiaki, H.; Amakawa, M.; Shimono, Y.; Tanikaga, R.; Holzwarth, A. R.; Schaffner, K. Synthetic Zinc and Magnesium Chlorin Aggregates as Models for Supramolecular Antenna Complexes in Chlorosomes of Green Photosynthetic Bacteria. *Photochem. Photobiol.* **1996**, *63* (1), 92–99. <https://doi.org/10.1111/j.1751-1097.1996.tb02997.x>.
- (43) Neuteboom, E. E.; Meskers, S. C. J.; Meijer, E. W.; Janssen, R. A. J. Photoluminescence of Self-Organized Perylene Bisimide Polymers. *Macromol. Chem. Phys.* **2004**, *205* (2), 217–222. <https://doi.org/10.1002/macp.200300044>.
- (44) Byrdin, M.; Jordan, P.; Krauss, N.; Fromme, P.; Stehlik, D.; Schlodder, E. Light Harvesting in Photosystem I: Modeling Based on the 2.5-Å Structure of Photosystem I from *Synechococcus Elongatus*. *Biophys. J.* **2002**, *83* (1), 433–457. [https://doi.org/10.1016/S0006-3495\(02\)75181-3](https://doi.org/10.1016/S0006-3495(02)75181-3).
- (45) Wang, X.-F.; Kitao, O.; Zhou, H.; Tamiaki, H.; Sasaki, S. Efficient Dye-Sensitized Solar Cell Based on Oxo-Bacteriochlorin Sensitizers with Broadband Absorption Capability. *J. Phys. Chem. C* **2009**, *113* (18), 7954–7961. <https://doi.org/10.1021/jp900328u>.

- (46) Das, A.; Danao, A.; Banerjee, S.; Raj, A. M.; Sharma, G.; Prabhakar, R.; Srinivasan, V.; Ramamurthy, V.; Sen, P. Dynamics of Anthracene Excimer Formation within a Water-Soluble Nanocavity at Room Temperature. *J. Am. Chem. Soc.* **2021**, *143* (4), 2025–2036. <https://doi.org/10.1021/jacs.0c12169>.
- (47) Pensack, R. D.; Ashmore, R. J.; Paoletta, A. L.; Scholes, G. D. The Nature of Excimer Formation in Crystalline Pyrene Nanoparticles. *J. Phys. Chem. C* **2018**, *122* (36), 21004–21017. <https://doi.org/10.1021/acs.jpcc.8b03963>.
- (48) Giaimo, J. M.; Lockard, J. V.; Sinks, L. E.; Scott, A. M.; Wilson, T. M.; Wasielewski, M. R. Excited Singlet States of Covalently Bound, Cofacial Dimers and Trimers of Perylene-3,4:9,10-Bis(Dicarboximide)s. *J. Phys. Chem. A* **2008**, *112* (11), 2322–2330. <https://doi.org/10.1021/jp710847q>.
- (49) Yoo, H.; Yang, J.; Yousef, A.; Wasielewski, M. R.; Kim, D. Excimer Formation Dynamics of Intramolecular π -Stacked Perylenediimides Probed by Single-Molecule Fluorescence Spectroscopy. *J. Am. Chem. Soc.* **2010**, *132* (11), 3939–3944. <https://doi.org/10.1021/ja910724x>.
- (50) Brown, K. E.; Salamant, W. A.; Shoer, L. E.; Young, R. M.; Wasielewski, M. R. Direct Observation of Ultrafast Excimer Formation in Covalent Perylenediimide Dimers Using Near-Infrared Transient Absorption Spectroscopy. *J. Phys. Chem. Lett.* **2014**, *5* (15), 2588–2593. <https://doi.org/10.1021/jz5011797>.
- (51) Bahsoun, H.; Chervy, T.; Thomas, A.; Börjesson, K.; Hertzog, M.; George, J.; Devaux, E.; Genet, C.; Hutchison, J. A.; Ebbesen, T. W. Electronic Light–Matter Strong Coupling in Nanofluidic Fabry–Pérot Cavities. *ACS Photonics* **2018**, *5* (1), 225–232. <https://doi.org/10.1021/acsphotonics.7b00679>.
- (52) Cho, I.; Kendrick, W. J.; Stuart, A. N.; Ramkissoon, P.; Ghiggino, K. P.; Wong, W. W. H.; Lakhwani, G. Multi-Resonance TADF in Optical Cavities: Suppressing Excimer Emission through Efficient Energy Transfer to the Lower Polariton States. *J. Mater. Chem. C* **2023**, *11* (41), 14448–14455. <https://doi.org/10.1039/D3TC02133E>.
- (53) Mony, J.; Yu, Y.; Schäfer, C.; Mallick, S.; Kushwaha, K.; Börjesson, K. Interplay between Polaritonic and Molecular Trap States. *J. Phys. Chem. C* **2022**, *126* (18), 7965–7972. <https://doi.org/10.1021/acs.jpcc.2c01239>.
- (54) George, J.; Wang, S.; Chervy, T.; Canaguier-Durand, A.; Schaeffer, G.; Lehn, J.-M.; Hutchison, J. A.; Genet, C.; Ebbesen, T. W. Ultra-Strong Coupling of Molecular Materials: Spectroscopy and Dynamics. *Faraday Discuss.* **2015**, *178* (0), 281–294. <https://doi.org/10.1039/C4FD00197D>.
- (55) Schwartz, T.; Hutchison, J. A.; Léonard, J.; Genet, C.; Haacke, S.; Ebbesen, T. W. Polariton Dynamics under Strong Light–Molecule Coupling. *ChemPhysChem* **2013**, *14* (1), 125–131. <https://doi.org/10.1002/cphc.201200734>.
- (56) Wang, S.; Chervy, T.; George, J.; Hutchison, J. A.; Genet, C.; Ebbesen, T. W. Quantum Yield of Polariton Emission from Hybrid Light-Matter States. *J. Phys. Chem. Lett.* **2014**, *5* (8), 1433–1439. <https://doi.org/10.1021/jz5004439>.
- (57) Coles, D. M.; Grant, R. T.; Lidzey, D. G.; Clark, C.; Lagoudakis, P. G. Imaging the Polariton Relaxation Bottleneck in Strongly Coupled Organic Semiconductor Microcavities. *Phys. Rev. B* **2013**, *88* (12), 121303. <https://doi.org/10.1103/PhysRevB.88.121303>.

- (58) Kéna-Cohen, S.; Maier, S. A.; Bradley, D. D. C. Ultrastrongly Coupled Exciton–Polaritons in Metal-Clad Organic Semiconductor Microcavities. *Adv. Opt. Mater.* **2013**, *1* (11), 827–833. <https://doi.org/10.1002/adom.201300256>.
- (59) Stanley, R. P.; Houdré, R.; Weisbuch, C.; Oesterle, U.; Ilegems, M. Cavity-Polariton Photoluminescence in Semiconductor Microcavities: Experimental Evidence. *Phys. Rev. B* **1996**, *53* (16), 10995–11007. <https://doi.org/10.1103/PhysRevB.53.10995>.
- (60) Houdré, R. Early Stages of Continuous Wave Experiments on Cavity-Polaritons. *Phys. Status Solidi B* **2005**, *242* (11), 2167–2196. <https://doi.org/10.1002/pssb.200560966>.
- (61) Wang, K.; Nagarajan, K.; Kushida, S.; Kulangara, S.; Genet, C.; Ebbesen, T. Study of the Selection Rules of Molecular Polaritonic Transitions by Two-Photon Absorption Spectroscopy.
- (62) Purcell, E. M. Spontaneous Emission Probabilities at Radio Frequencies. In *Confined Electrons and Photons: New Physics and Applications*; Burstein, E., Weisbuch, C., Eds.; NATO ASI Series; Springer US: Boston, MA, 1995; pp 839–839. https://doi.org/10.1007/978-1-4615-1963-8_40.
- (63) Valeur, B. Front Matter and Index. In *Molecular Fluorescence*; John Wiley & Sons, Ltd, 2001; pp i–xiv. https://doi.org/10.1002/3527600248.fmatter_indsub.
- (64) Castagnola, M.; Haugland, T. S.; Ronca, E.; Koch, H.; Schäfer, C. Collective Strong Coupling Modifies Aggregation and Solvation. *J. Phys. Chem. Lett.* **2024**, *15* (5), 1428–1434. <https://doi.org/10.1021/acs.jpcclett.3c03506>.
- (65) Piejko, M.; Patrahau, B.; Joseph, K.; Muller, C.; Devaux, E.; Ebbesen, T. W.; Moran, J. Solvent Polarity under Vibrational Strong Coupling. *J. Am. Chem. Soc.* **2023**, *145* (24), 13215–13222. <https://doi.org/10.1021/jacs.3c02260>.
- (66) Zhong, C.; Hou, S.; Zhao, X.; Bai, J.; Wang, Z.; Gao, F.; Guo, J.; Zhang, F. Driving DNA Origami Coassembling by Vibrational Strong Coupling in the Dark. *ACS Photonics* **2023**, *10* (5), 1618–1623. <https://doi.org/10.1021/acsphotonics.3c00235>.
- (67) Schäfer, C.; Fojt, J.; Lindgren, E.; Erhart, P. Machine Learning for Polaritonic Chemistry: Accessing Chemical Kinetics. *J. Am. Chem. Soc.* **2024**. <https://doi.org/10.1021/jacs.3c12829>.
- (68) Thomas, A.; Devaux, E.; Nagarajan, K.; Rogez, G.; Seidel, M.; Richard, F.; Genet, C.; Drillon, M.; Ebbesen, T. W. Large Enhancement of Ferromagnetism under a Collective Strong Coupling of YBCO Nanoparticles. *Nano Lett.* **2021**, *21* (10), 4365–4370. <https://doi.org/10.1021/acs.nanolett.1c00973>.
- (69) Jarc, G.; Mathengattil, S. Y.; Montanaro, A.; Giusti, F.; Rigoni, E. M.; Sergo, R.; Fassoli, F.; Winnerl, S.; Dal Zilio, S.; Mihailovic, D.; Prelovšek, P.; Eckstein, M.; Fausti, D. Cavity-Mediated Thermal Control of Metal-to-Insulator Transition in 1T-TaS₂. *Nature* **2023**, *622* (7983), 487–492. <https://doi.org/10.1038/s41586-023-06596-2>.
- (70) Kumar, S.; Biswas, S.; Rashid, U.; Mony, K. S.; Chandrasekharan, G.; Mattiotti, F.; Vergauwe, R. M. A.; Hagenmuller, D.; Kaliginedi, V.; Thomas, A. Extraordinary Electrical Conductance through Amorphous Non-Conducting Polymers under Vibrational Strong Coupling. arXiv December 13, 2023. <https://doi.org/10.48550/arXiv.2303.03777>.